Journal of Power, Energy, and Control

Research article

Solidification Process Investigation of LiCl Salt as PCM with Temperature-Dependent Density and Viscosity by Enthalpy Porosity Simulation Model

Nur Syah Ibrahim[1], Alief Avicenna Luthfie[1,2*]

[1] Mechanical Engineering Study Program, Faculty of Engineering, Universitas Mercu Buana, Jakarta, Indonesia

[2] Department of Mechanical Engineering, Graduate School of Science and Engineering, Chiba University, Chiba, Japan

*Correspondence: alief.avicenna@mercubuana.ac.id

https://doi.org/10.62777/pec.v2i1.42

Received: 31 October 2024
Revised: 23 March 2025
Accepted: 29 March 2025
Published: 18 April 2025

Abstract: An enthalpy porosity simulation model is widely used to simulate the solidification process of a Phase Change Material (PCM) with constant density and viscosity. Consequently, numerical inaccuracy may arise in the investigation of the solidification process. Therefore, this study investigates the solidification of lithium chloride (LiCl) as a PCM, incorporating temperature-dependent density and viscosity in the enthalpy porosity model. Furthermore, the computational domain is represented by a concentric pipe, with the LiCl salt assumed to be fully filled within the annulus. The boundary conditions are adiabatic on the outer radius and constant temperature on the inner radius, representing the temperature of the Heat Transfer Fluid (HTF). The simulation results show that the solidification process with temperature-dependent density and viscosity required a total time of 2360 s to complete the solidification process. In addition, the solidification rate is decreased at the beginning of the solidification process and then increased before being decreased at the end of the solidification process. Furthermore, a comparison is conducted with constant density and viscosity. The comparison result shows that the solidification time of temperature-dependent density and viscosity is shorter than the solidification process time of constant density and viscosity with a deviation of 8.5%, indicating the importance of using the temperature-dependent density and viscosity to investigate the solidification time. Conversely, the solidification rate shows a similar tendency, indicating the insignificant effect of using the temperature-dependent density and viscosity to investigate the solidification rate.

Keywords: Solidification process, LiCl salt, PCM, enthalpy porosity simulation model, temperature-dependent density and viscosity

1. Introduction

In response to worldwide energy and environmental issues, replacing conventional fossil fuel-based energy conversion technologies with more efficient renewable energy has become a global priority in recent years [1], [2]. For instance, the utilization of a

concentrated solar thermal (CST) plant to collect thermal energy from the solar system. To store excess energy, a shell and tube latent thermal energy storage (LHTES) is usually integrated into the CST plant. The LHTES utilizes phase change materials (PCMs) to store the thermal energy in the form of latent heat from the solar system through a charging process. This stored energy can then be released to provide stable heat through a discharging process [3]. Recently, salt has been widely used as PCM due to its excellent chemical stability, high energy storage density, etc. [4], [5]. During the discharging process, salt as PCM in the shell and tube LHTES releases the latent heat to a heat transfer fluid (HTF) with a lower temperature. Consequently, the salt undergoes a solidification process from the liquid phase to the solid phase [6], [7]. During the phase change process, the density and viscosity of the salt change continuously according to the temperature of the salt. Hence, creating a fluctuated solidification time and rate, which results in the alteration of the efficiency of the salt as PCM. Therefore, a solidification process investigation of salt as PCM with temperature-dependent density and viscosity is highly needed in order to be able to predict the efficiency of a salt as PCM.

A number of experimental studies on a TES during the solidification process were conducted by several researchers [8]. For instance, an investigation of the performance of a shell and tube TES [9], and a study of the different types of materials for the applications of PCMs [10]. However, the experimental study of salt solidification requires a lot of cost and time. Consequently, a cheaper and practical method is needed. One of which is the simulation method by utilizing enthalpy porosity simulation model. In the enthalpy porosity simulation model, the solidification process is modeled by enthalpy changes as well as porosity changes due to a decrease in the liquid fraction. However, the use of this model is still focused on the constant density and viscosity of the PCM [11], [12], [13]. Although numerous studies employ constant density and viscosity, only a few consider the effects of temperature-dependent properties on solidification behavior in PCMs. Consequently, numerical inaccuracy may arise in the investigation because the constant density and viscosity do not sufficiently represent the change in the density and viscosity in terms of temperature.

Therefore, the present work aims to investigate the solidification process of a salt as PCM with temperature-dependent density and viscosity by utilizing the enthalpy porosity simulation model. To demonstrate the temperature-dependent density and viscosity, lithium chloride (LiCl) is selected as the salt for the PCM. The investigation can be divided into two parts: 1) the investigation of the solidification time, and 2) the investigation of the solidification rate, which is defined as the decreasing of liquid fraction per unit time. Moreover, this present work also compares the solidification time and rate between the ones with temperature-dependent density and viscosity, and the ones with constant density and viscosity.

2. Methods

The solidification process of LiCl salt as PCM is started in the liquid phase by releasing latent heat to the surrounding area. Consequently, the total enthalpy of LiCl salt decreases. This condition leads to the appearance of crystal nuclei. Consequently, the liquid and solid phases coexist to form a mushy zone [14]. If the solidification process continues, crystal nuclei coagulate to form a larger crystal. In this situation, a resistive force within the mushy zone, *i.e.,* the mushy force $\vec{\mathbf{F}}_{\mathrm{Mush}}$ serves to dampen the momentum inside the LiCl salt.

In the present work, the solidification process of LiCl salt as PCM is investigated by the enthalpy porosity simulation model with temperature-dependent density $\rho(T)$ and

viscosity $\mu(T)$as depicted in Figure 1. In the enthalpy porosity simulation model, the solidification process is modeled by enthalpy changes and porosity changes, which is represented by the liquid mass fraction φ_{L} transition (from $\varphi_{\mathrm{L}} = 1$ to $\varphi_{\mathrm{L}} = 0$) in the $\vec{\mathbf{F}}_{\mathrm{Mush}}$. After the φ_{L} transition is obtained, the solidification process is investigated according to the solidification time t_{S} and the solidification rate ξ.

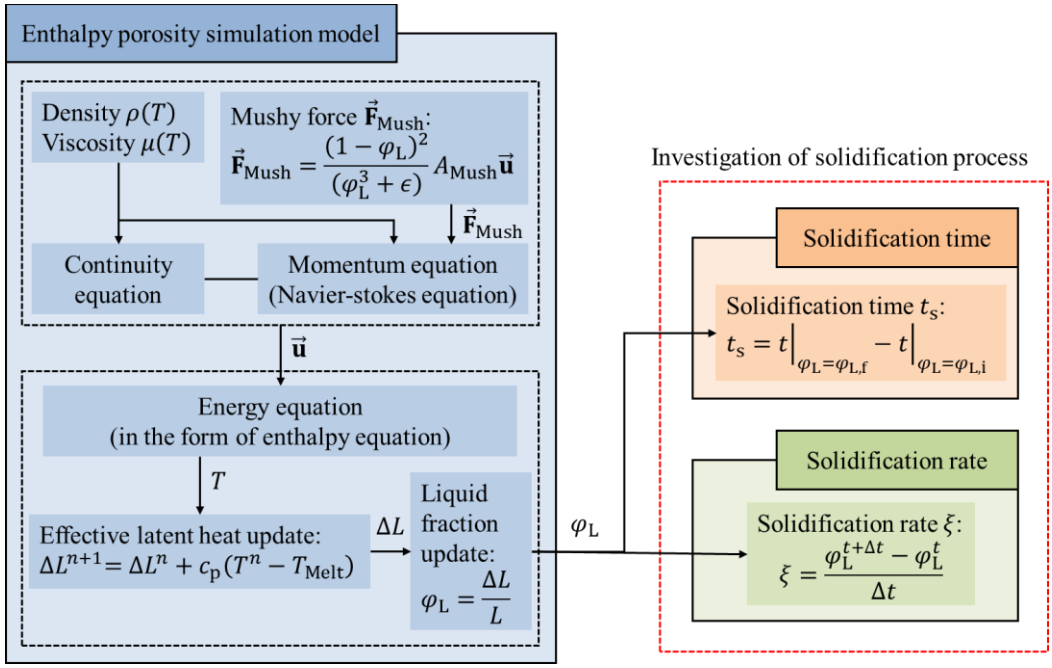

Figure 1. Investigation of solidification process by enthalpy porosity model.

2.1. Mathematical Model

As presented in Figure 1, three governing equations are utilized to simulate the φ_{L} transition during the solidification process, *i.e.*, continuity, momentum, and energy equations. The continuity and momentum equation, which are derived from Navier Stokes' equation, are utilized to obtain velocity vector $\vec{\mathbf{u}}$ within the LiCl salt according to the $\rho(T)$ and the $\mu(T)$. Both continuity and momentum are calculated simultaneously during the simulation. The continuity and momentum equation are expressed as follows [15].

$$\frac{\partial}{\partial t}\rho(T) + \vec{\nabla}\cdot[\rho(T)\vec{\mathbf{u}}] = 0 \tag{1}$$

$$\frac{\partial}{\partial t}(\rho(T)\vec{\mathbf{u}}) + \vec{\nabla}\cdot[\rho(T)\vec{\mathbf{u}}\vec{\mathbf{u}}] = -\vec{\nabla}P + \vec{\nabla}\cdot\mu(T)\left(\vec{\nabla}\vec{\mathbf{u}} + \vec{\nabla}\vec{\mathbf{u}}^{\mathrm{T}}\right) + \rho(T)\vec{\mathbf{g}} + \vec{\mathbf{F}}_{\mathrm{Mush}} \tag{2}$$

$$\vec{\mathbf{F}}_{\mathrm{Mush}} = \frac{(1-\varphi_{\mathrm{L}})^2}{(\varphi_{\mathrm{L}}^3+\epsilon)} A_{\mathrm{Mush}}\vec{\mathbf{u}} \tag{3}$$

where P is pressure within the LiCl salt, $\vec{\mathbf{g}}$ is gravitational acceleration vector, A_{Mush} is mushy zone constant which is preferably 10^3 and 10^7 [16], and ϵ is small number (0.001) to prevent error during the simulation in the case $\varphi_{\mathrm{L}} = 0$. During the solidification process, the φ_{L} changes from 1 to 0. Consequently, the $\vec{\mathbf{F}}_{\mathrm{Mush}}$ becomes very large during the solidification process. Thereby, the momentum is dampened and the $\vec{\mathbf{u}}$ is decreased.

The third governing equation is the energy equation. As presented in Figure 1, the energy equation utilizes the $\vec{\mathbf{u}}$ obtained from the simultaneous calculation of continuity and momentum. The energy equation is expressed as follows [15]:

$$\frac{\partial}{\partial t}(\rho(T)h) + \vec{\nabla} \cdot (\rho(T)\vec{\mathbf{u}}h) = \vec{\nabla} \cdot \left(k\vec{\nabla}T\right) \tag{4}$$

where h is total enthalpy of the LiCl salt, k is constant thermal conductivity of LiCl salt, and T is temperature of LiCl salt. The h in Equation (4) is the sum of sensible enthalpy and latent enthalpy which can be expressed as:

$$h = h_{\mathrm{Ref}} + c_{\mathrm{p}} \int_{T_{\mathrm{Ref}}}^{T} \mathrm{d}T + \Delta L \tag{5}$$

where c_{p} is constant specific heat of LiCl, T_{Ref} is reference temperature, h_{Ref} is reference enthalpy which is calculated at the T_{Ref}, and ΔL is effective latent heat. In the simulation which utilizes pure material, the ΔL is updated as follows [17]:

$$\Delta L^{n+1} = \Delta L^{n} + c_{\mathrm{p}}(T^{n} - T_{\mathrm{Melt}}) \tag{6}$$

where T_{Melt} is melting temperature of LiCl and superscript n is iteration number. During the solidification process, the ΔL changes from L to 0. In this case, L is constant latent heat of LiCl. After the ΔL is obtained, the φ_{L} can be obtained from [18]

$$\varphi_{\mathrm{L}} = \frac{\Delta L}{L} \tag{7}$$

2.2. Investigation of Solidification Process

Figure 1 shows that the investigation process includes the investigation of solidification time t_{S} and rate ξ. This process is based on the φ_{L} obtained from the enthalpy porosity simulation model. The t_{S} is defined as the total time needed for the solidification process to be completed. Therefore, the t_{S} can be calculated as follows:

$$t_{\mathrm{s}} = t|_{\varphi_{\mathrm{L}}=\varphi_{\mathrm{L,f}}} - t|_{\varphi_{\mathrm{L}}=\varphi_{\mathrm{L,i}}} \tag{8}$$

where $t|_{\varphi_{\mathrm{L}}=\varphi_{\mathrm{L,f}}}$ is the final time when the solidification process is completed and $t|_{\varphi_{\mathrm{L}}=\varphi_{\mathrm{L,i}}}$ is the initial time when the solidification process is started.

Furthermore, the ξ is defined as the decreasing of liquid fraction per unit time. Mathematically, the ξ can be calculated as follows:

$$\xi = \frac{\varphi_{\mathrm{L}}^{t+\Delta t} - \varphi_{\mathrm{L}}^{t}}{\Delta t} \tag{9}$$

where Δt is time difference. Moreover, the φ_{L}^{t} is the φ_{L} at time t and $\varphi_{\mathrm{L}}^{t+\Delta t}$ is the φ_{L} at time $t + \Delta t$.

2.3. Simulation Model Conditions

As described in Section 2.1, the density and viscosity of LiCl salt in the present work are defined as temperature-dependent density $\rho(T)$ and viscosity $\mu(T)$. The temperature-dependent density $\rho(T)$ and viscosity $\mu(T)$ are expressed as [19]:

$$\rho(T) = 2.1359 - 5.831 \times 10^{-4}T \tag{10}$$

$$\mu(T) = 7{,}32 \times 10^{-2} \exp\left(\frac{5601.7}{RT}\right) \tag{11}$$

where R is universal gas constant ($= 8.314\ \mathrm{J/mol \cdot K}$). Figure 2 shows the comparison between constant values and temperature-dependent values of density and viscosity.

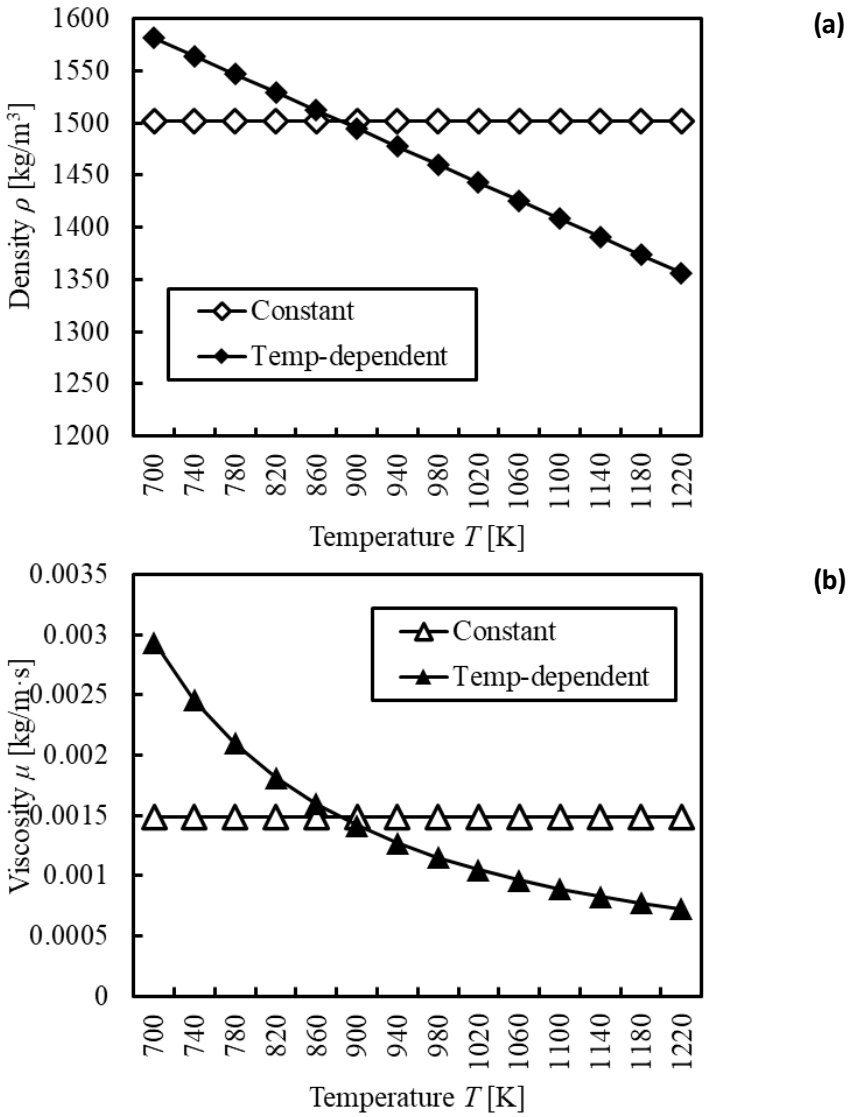

Figure 2. Comparison between constant values and temperature-dependent values of **(a)** density and **(b)** viscosity.

According to Section 1, this present work also compares the solidification time and rate between the ones with temperature-dependent density $\rho(T)$ and viscosity $\mu(T)$, and the ones with constant density and viscosity. In the simulation with constant density and viscosity, the gravitational effect and density change is represented by the Boussinesq approximation [20]. Table 1 shows the constant physical and thermal properties which are utilized in the present work.

Table 1. Physical and thermal properties of LiCl salt.

Properties	Symbol	Value	Unit	Ref.
Density	ρ	1502	kg/m^3	[21]
Specific Heat	c_p	1534	J/kg·K	[21]
Thermal Conductivity	k	1.5098	W/m·K	[21]
Viscosity	μ	0.001487	kg/m·s	[21]
Thermal Expansion Coefficient		0.000287	1/K	[22]
Latent Heat	L	470094	J/kg	[21]
Melting Temperature	T_Melt	883	K	[21]

2.3. Computational Domain and Boundary Conditions

To demonstrate the use of LiCl salt as PCM in the shell and tube LHTES, the computational domain in the present work is defined as a concentric tube where the LiCl salt is located in the outer pipe or annulus and the HTF flows in the inner cylinder [23]. However, in this present work, the inner cylinder is excluded from the computational domain. Hence, the effect of HTF is represented by the constant temperature at the inner radius [22]. Consequently, the computational domain and its respective boundary conditions can be shown in Figure 3. According to Figure 3, the computational domain has total length of $z = 500$ mm and its outer r_o and inner r_i diameter are $r_o = 56.15$ mm and $r_i = 24.13$ mm, respectively. Moreover, the boundary conditions can be divided into three, which are adiabatic condition, no slip condition, and temperature condition. The adiabatic condition is located at $r = r_o$ and expressed as:

$$\vec{\mathbf{q}}\big|_{r=r_o} = \frac{\mathrm{d}T}{\mathrm{d}r}\bigg|_{r=r_o} = 0 \ \mathrm{W/m^2} \tag{12}$$

where $\vec{\mathbf{q}}$ is heat flux. The adiabatic condition is specified to ensure that the latent heat transfer occurs solely to the HTF in the inner radius.

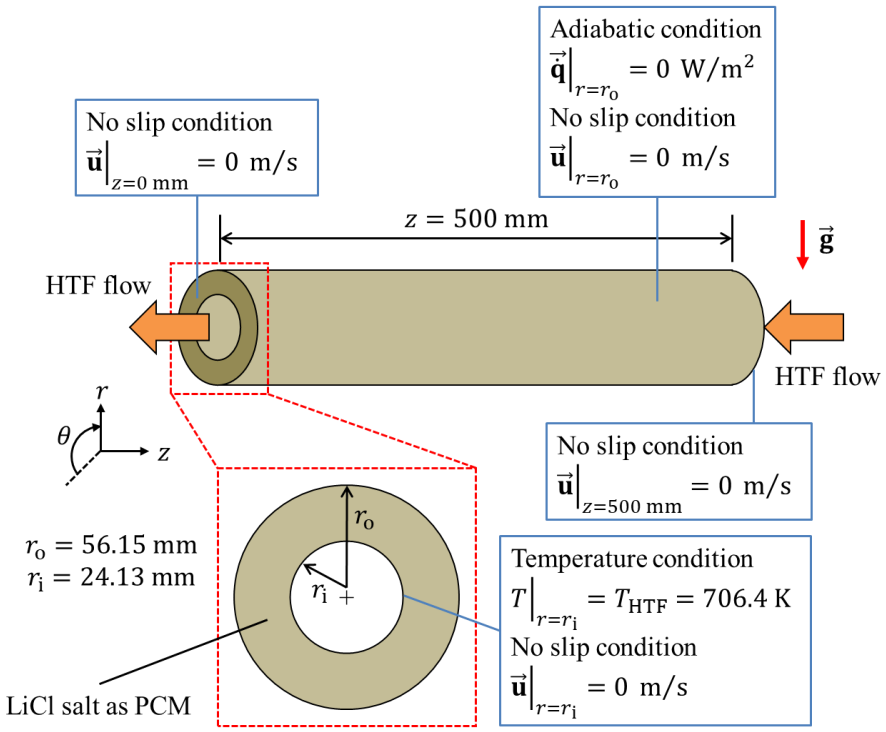

Figure 3. Computational domain and boundary conditions.

Additionally, no-slip conditions are identified at various points, which are $r = r_o$, $r = r_i$, $z = 0$ mm, and $z = 500$ mm. The no-slip conditions occurred due to the contact between LiCl salt as PCM and its container wall. Furthermore, these conditions are specified to ensure that small layer of LiCl salt as PCM has no velocity relative to its container wall. Therefore, these conditions are expressed as follows:

$$\vec{\mathbf{u}}|_{r=r_o} = 0 \ \mathrm{m/s} \tag{13}$$

$$\vec{\mathbf{u}}|_{r=r_i} = 0 \ \mathrm{m/s} \tag{14}$$

$$\vec{\mathbf{u}}|_{z=0\ \mathrm{mm}} = 0\ \mathrm{m/s} \tag{15}$$

$$\vec{\mathbf{u}}|_{z=500\ \mathrm{mm}} = 0\ \mathrm{m/s} \tag{16}$$

Finally, the temperature condition which is located at $r = r_{\mathrm{i}}$ is specified to address the involvement of the HTF in the solidification process in terms of its temperature. In the present work, the HTF is solely responsible for the latent heat loss from the LiCl salt as PCM. The temperature of the HTF T_{HTF} is specified as a temperature below the melting temperature of LiCl salt as PCM ($T_{\mathrm{Melt}} = 883\ \mathrm{K}$) to ensure that the heat transfer occurs from the LiCl salt as PCM to the HTF in the inner radius. Therefore, the temperature condition is determined as:

$$T|_{r=r_{\mathrm{i}}} = T_{\mathrm{HTF}} = 706.4\ \mathrm{K} \tag{17}$$

In addition to boundary conditions, the initial conditions are specified because the simulation of the solidification process by the enthalpy porosity simulation model is a time-dependent process (transient). In the simulation, the total time is 3000 s with time step size is $\Delta t = 1\mathrm{s}$. In the present work, the initial conditions are specified as a temperature which is higher than the melting temperature of the LiCl salt as PCM ($T_{\mathrm{Melt}} = 883\ \mathrm{K}$) to ensure that the LiCl salt as PCM is in the liquid phase. Hence, the initial conditions are determined as:

$$T|_{t=0} = 905.075\ \mathrm{K} \tag{18}$$

$${}^{\mathrm{L}}\varphi\big|_{t=0} = 1 \tag{19}$$

Before the simulation of the solidification process is started, the computational domain shown in Figure 3 is discretized by hexahedral meshes. The generated mesh is shown in Figure 4. The discretization scheme is structured with the characteristics shown in Table 2.

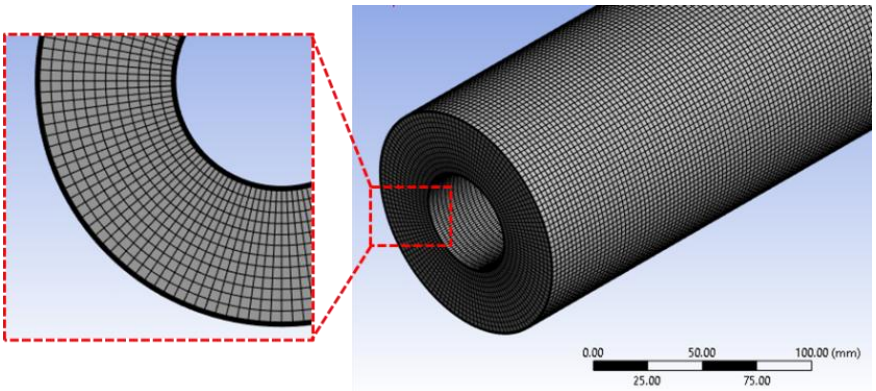

Figure 4. Discretized computational domain.

Table 2. Discretization characteristics.

Characteristics	Values [-]
Number of elements	623000
Number of nodes	652000
Average skewness	0.018431

3. Results and Discussion

3.1. Solidification Time

The solidification process of LiCl salt as PCM is simulated by the enthalpy porosity simulation model with temperature-dependent density and viscosity and investigated according to its solidification time t_s. In order to obtain the t_s, the liquid mass fraction φ_L transition of LiCl salt as PCM during the solidification process must be determined in the first place. As the results of the simulation, the φ_L transition is shown in Figure 5. As shown in Figure 5, at the start of the solidification process, the φ_L is equal to 0.72. This is because there is solid phase at $t = 0$ as the results of the HTF temperature in the inner radius. In this case, the $t|_{\varphi_L=\varphi_{L,i}}$ is defined as the time when $\varphi_L = 0.72$ and $t|_{\varphi_L=\varphi_{L,f}}$ is defined as the time when $\varphi_L = 0$. Therefore, the solidification time with temperature-dependent density and viscosity $t_{s,dep}$ according to Equation 8 is 2360 s.

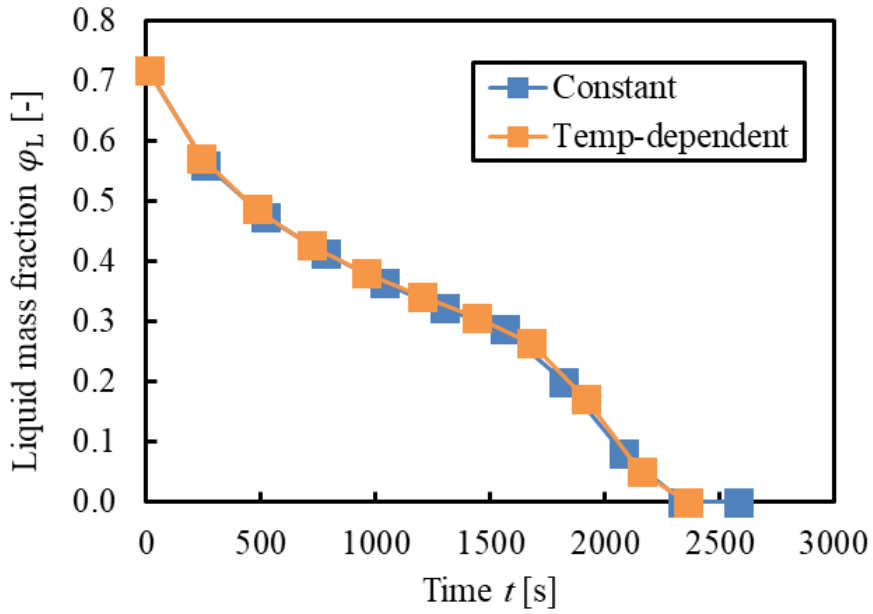

Figure 5. Transition of liquid mass fraction φ_L during solidification process of LiCl salt as PCM.

Figure 5 also shows the φ_L transition of LiCl salt as PCM with constant density and viscosity. Similar to the one with temperature-dependent density and viscosity, the φ_L transition with constant density and viscosity is started at $\varphi_L = 0.72$. In this case, the $t|_{\varphi_L=\varphi_{L,i}}$ is defined as the time when $\varphi_L = 0.72$ and $t|_{\varphi_L=\varphi_{L,f}}$ is defined as the time when $\varphi_L = 0$. Therefore, in the case of constant density and viscosity, the solidification time with constant density and viscosity $t_{s,cons}$ according to Equation 8 is 2580 s.

The direct comparison between the $t_{s,dep}$ and the $t_{s,cons}$ shows that the $t_{s,dep}$ is shorter than the $t_{s,cons}$. Consequently, the solidification time is faster when the temperature-dependent density and viscosity is included. This faster solidification time indicates that the nucleation of LiCl salt as PCM with temperature-dependent density and viscosity occurs more rapidly than LiCl salt as PCM with constant density and viscosity. This is because in its metastable state, the one with temperature-dependent density and viscosity is further away from the stable state compared to the one with constant density and viscosity [21], [24]. A similar phenomenon is observed in reference [22].

In order to evaluate the solidification time, deviation δ_t between the $t_{s,dep}$ and the $t_{s,cons}$ is defined as:

$$\delta_t = \frac{\left|t_{\mathrm{s,dep}} - t_{\mathrm{s,cons}}\right|}{t_{\mathrm{s,cons}}} \times 100\% \tag{20}$$

Therefore, the δ_t is 8.5% which suggest that the temperature-dependent density and viscosity has a significant effect on altering the solidification time. Consequently, it is not recommended to ignore the temperature density and viscosity in the simulation of solidification process.

3.2. Solidification Rate

In the present work, solidification rate ξ is also investigated based on the φ_{L} transition of LiCl salt as PCM during the solidification process. As shown in Equation 9, the ξ is defined as the decreasing φ_{L} per unit time. According to the φ_{L} transition shown in Figure 5, the ξ is shown in Figure 6.

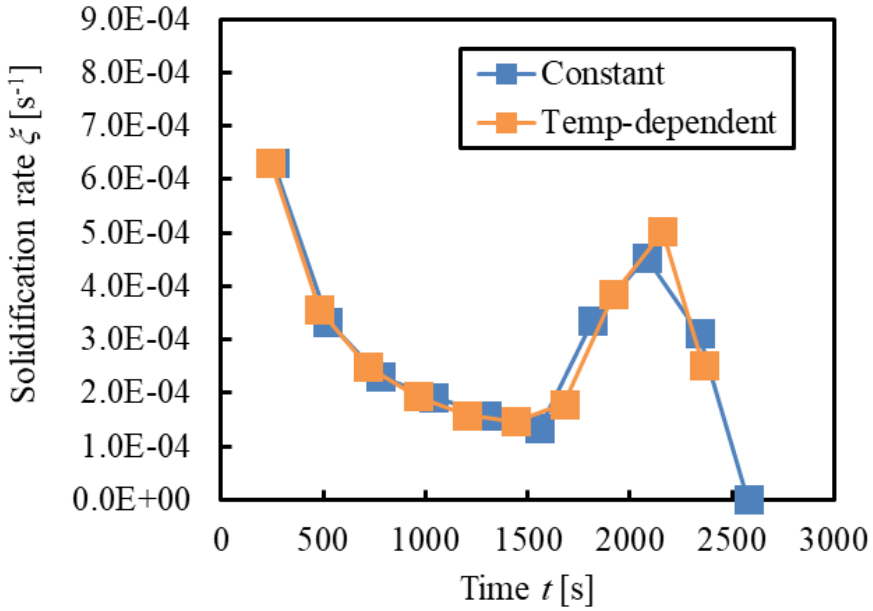

Figure 6. Solidification rate ξ during solidification process of LiCl salt as PCM.

In the case of solidification rate ξ, the ξ is decreasing until $t = 1440$ s. After that, the ξ is increasing until $t = 2160$ s. Finally, the ξ is decreasing until $t = 2360$ s. The decreasing ξ indicates that the formation of solid phase is slower over the time, while the increasing ξ indicates that the formation of solid phase is faster over the time. During the decreasing ξ, the mushy zone, *i.e.*, the zone where liquid phase and solid phase coexists, still persists in encircling the computational domain. Furthermore, during the increasing ξ, the remaining mushy zone is shifted upward (in the opposite direction of the gravity), while the solid phase is shifted downward (in the same direction of the gravity) due to the high density of the solid phase. At the end of the solidification process, the decreasing ξ occurs because only a thin layer of mushy zone is remaining during $t = 2160$ s until $t = 2360$ s. The visualization of the φ_{L} to describe the position of mushy zone during the solidification process is depicted in Figure 7.

In Figure 7, the visualization of the φ_{L} is shown in three designated plane (plane 1 is located at $z = 100$ mm, plane 2 is located at $z = 250$ mm, and plane 3 is located at $z = 500$ mm. According to Figure 7, the solid phase emerges from the inner radius of the computational domain, where the HTF is flowing. This phenomenon shows that the heat transfer only occurs from the LiCl salt to the HTF. Therefore, the latent heat only travels from the LiCl salt to the HTF. In addition, during the solidification process, the viscosity of LiCl salt increases as shown in Figure 2, resulting in an increase in the shear stress of the

LiCl salt. The increase in shear stress causes the LiCl salt particles to move with less freedom, thus creating a homogeneous distribution as depicted in Figure 7.

Furthermore, the ξ of LiCl salt as PCM with constant density and viscosity is also shown in Figure 6. According to Figure 6, the ξ of LiCl salt as PCM with temperature-dependent density and viscosity and LiCl salt as PCM with constant density and viscosity shows similar tendency. In the case of constant density and viscosity, the density difference between the solid phase and the remaining phase is represented by the Boussinesq approximation. Consequently, the use of temperature-dependent density and viscosity has insignificant effect in the investigation of the ξ.

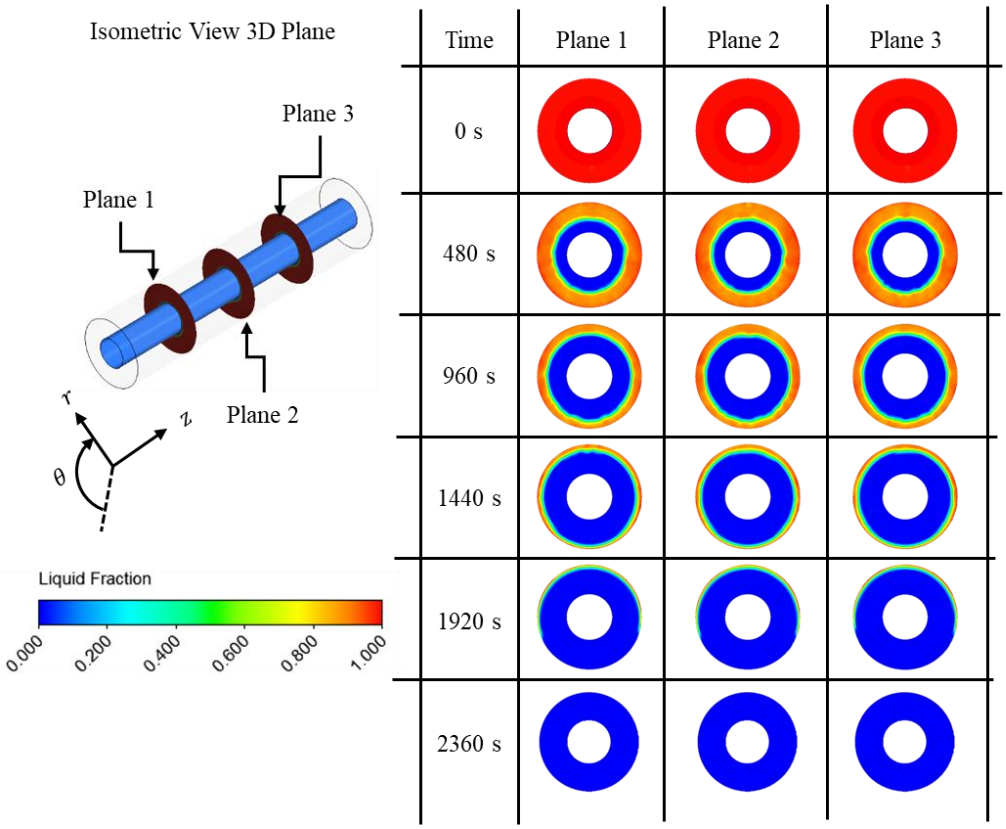

Figure 7. Visualization of liquid mass fraction φ_{L} during solidification process of LiCl salt as PCM.

4. Conclusion

In the present work, the solidification process of the LiCl salt as PCM with temperature-dependent density and viscosity is investigated by the enthalpy porosity simulation model. The investigation is divided into 1) the investigation of the solidification time t_{s}, and 2) the investigation of the solidification rate ξ. According to the results and discussion, the conclusions are:

1. The solidification process of LiCl salt as PCM with temperature-dependent physical density and viscosity has been successfully simulated by the enthalpy porosity simulation model. The results shows that the solidification time t_{s} is 2360 s. This solidification time is shorter compared to the one with constant density and viscosity. The deviation between the one with temperature-dependent density and viscosity and the one with constant density and viscosity is 8.5%. This deviation suggests that it is not recommended to ignore the temperature density and viscosity in the simulation of solidification process.
2. The solidification rate ξ shows decreasing at the beginning of the solidification process until $t = 1440$ s, following the increasing until $t = 2160$ s, and decreasing until the end of the solidification process. The comparison with the LiCl salt as PCM

with constant density and viscosity shows similar tendency. Therefore, it suggests that the use of temperature-dependent density and viscosity has insignificant effect in the investigation of the ξ.

Funding: This research received no external funding.

Conflicts of Interest: The authors declare no conflicts of interest.

References

[1] N. Boerema, G. Morrison, R. Taylor, and G. Rosengarten, "High temperature solar thermal central-receiver billboard design," *Solar Energy*, vol. 97, pp. 356–368, Nov. 2013, doi: 10.1016/j.solener.2013.09.008.

[2] T. M. Pavlović, I. S. Radonjić, D. D. Milosavljević, and L. S. Pantić, "A review of concentrating solar power plants in the world and their potential use in Serbia," *Renewable and Sustainable Energy Reviews*, vol. 16, no. 6, pp. 3891–3902, Aug. 2012, doi: 10.1016/j.rser.2012.03.042.

[3] H. L. Zhang, J. Baeyens, J. Degrève, and G. Cacères, "Concentrated solar power plants: Review and design methodology," *Renewable and Sustainable Energy Reviews*, vol. 22, pp. 466–481, Jun. 2013, doi: 10.1016/j.rser.2013.01.032.

[4] S. Zhang, Y. Jin, and Y. Yan, "Depression of melting point and latent heat of molten salts as inorganic phase change material: Size effect and mechanism," *J Mol Liq*, vol. 346, p. 117058, Jan. 2022, doi: 10.1016/j.molliq.2021.117058.

[5] S. Zhang and Y. Yan, "Melting and thermodynamic properties of nanoscale binary chloride salt as high-temperature energy storage material," *Case Studies in Thermal Engineering*, vol. 25, p. 100973, Jun. 2021, doi: 10.1016/j.csite.2021.100973.

[6] D. Han, B. Guene Lougou, Y. Xu, Y. Shuai, and X. Huang, "Thermal properties characterization of chloride salts/nanoparticles composite phase change material for high-temperature thermal energy storage," *Appl Energy*, vol. 264, p. 114674, Apr. 2020, doi: 10.1016/j.apenergy.2020.114674.

[7] Vikas, A. Yadav, and S. K. Soni, "Simulation of Melting Process of a Phase Change Material (PCM) using ANSYS (Fluent)," *International Research Journal of Engineering and Technology (IRJET)*, vol. 4, no. 5, pp. 3289–3294, May 2017.

[8] H. A. Adine and H. El Qarnia, "Numerical analysis of the thermal behaviour of a shell-and-tube heat storage unit using phase change materials," *Appl Math Model*, vol. 33, no. 4, pp. 2132–2144, Apr. 2009, doi: 10.1016/j.apm.2008.05.016.

[9] S. Arena, G. Cau, and C. Palomba, "CFD Simulation of Melting and Solidification of PCM in Thermal Energy Storage Systems of Different Geometry," *J Phys Conf Ser*, vol. 655, p. 012051, Nov. 2015, doi: 10.1088/1742-6596/655/1/012051.

[10] M. Medrano, A. Gil, I. Martorell, X. Potau, and L. F. Cabeza, "State of the art on high-temperature thermal energy storage for power generation. Part 2—Case studies," *Renewable and Sustainable Energy Reviews*, vol. 14, no. 1, pp. 56–72, Jan. 2010, doi: 10.1016/j.rser.2009.07.036.

[11] S. Zhang and Y. Yan, "Evaluation of discharging performance of molten salt/ceramic foam composite phase change material in a shell-and-tube latent heat thermal energy storage unit," *Renew Energy*, vol. 198, pp. 1210–1223, Oct. 2022, doi: 10.1016/j.renene.2022.08.124.

[12] F. Fornarelli *et al.*, "Numerical simulation of a complete charging-discharging phase of a shell and tube thermal energy storage with phase change material," *Energy Procedia*, vol. 126, pp. 501–508, Sep. 2017, doi: 10.1016/j.egypro.2017.08.220.

[13] K. Hirai, S. Bellan, K. Matsubara, T. Kodama, N. Gokon, and H. S. Cho, "Numerical analysis on solidification process of PCM in triplex-tube thermal energy storage system," in *SOLARPACES 2019: International Conference on Concentrating Solar Power and Chemical Energy Systems*, Daegu: AIP, 2020, p. 190018. doi: 10.1063/5.0028873.

[14] D. V. Alexandrov, "Nucleation and growth of crystals at the intermediate stage of phase transformations in binary melts," *Philos Mag Lett*, vol. 94, no. 12, pp. 786–793, Dec. 2014, doi: 10.1080/09500839.2014.977975.

[15] K. Kant, A. Shukla, A. Sharma, and P. H. Biwole, "Melting and solidification behaviour of phase change materials with cyclic heating and cooling," *J Energy Storage*, vol. 15, pp. 274–282, Feb. 2018, doi: 10.1016/j.est.2017.12.005.

[16] A. Shahsavar, A. H. Majidzadeh, R. B. Mahani, and P. Talebizadehsardari, "Entropy and thermal performance analysis of PCM melting and solidification mechanisms in a wavy channel triplex-tube heat exchanger," *Renew Energy*, vol. 165, pp. 52–72, Mar. 2021, doi: 10.1016/j.renene.2020.11.074.

[17] W. D. Bennon and F. P. Incropera, "A continuum model for momentum, heat and species transport in

binary solid-liquid phase change systems—I. Model formulation," *Int J Heat Mass Transf*, vol. 30, no. 10, pp. 2161–2170, Oct. 1987, doi: 10.1016/0017-9310(87)90094-9.

[18] F. Li, A. Almarashi, M. Jafaryar, M. R. Hajizadeh, and Y.-M. Chu, "Melting process of nanoparticle enhanced PCM through storage cylinder incorporating fins," *Powder Technol*, vol. 381, pp. 551–560, Mar. 2021, doi: 10.1016/j.powtec.2020.12.026.

[19] G. J. Janz, F. W. Dampier, G. R. Lakshminarayanan, P. K. Lorenz, and R. P. T. Tomkins, "Molten Salts: Volume 1, Electrical Conductance, Density, and Viscosity Data," Washington D.C., NSRDS-NBS 15, 1968.

[20] M. Kirincic, A. Trp, and K. Lenic, "Influence of natural convection during melting and solidification of paraffin in a longitudinally finned shell-and-tube latent thermal energy storage on the applicability of developed numerical models," *Renew Energy*, vol. 179, pp. 1329–1344, Dec. 2021, doi: 10.1016/j.renene.2021.07.083.

[21] V. Shivam, S. Kar, G. K. Mandal, N. K. Mukhopadhyay, and V. C. Srivastava, "Microstructural design opportunities and phase stability in the spray-formed AlCoCr0.75Cu0.5FeNi high entropy alloy," *Journal of Alloys and Metallurgical Systems*, vol. 8, p. 100138, Dec. 2024, doi: 10.1016/j.jalmes.2024.100138.

[22] M. M. Hasan and A. A. Luthfie, "Melting Process Investigation of KCl Salt as a PCM by Enthalpy-Porosity Simulation Model with Temperature-dependent Physical Properties," *Journal of Power, Energy, and Control*, vol. 1, no. 2, pp. 58–67, Sep. 2024, doi: 10.62777/pec.v1i2.22.

[23] D. W. Green and M. Z. Southard, *Perry's Chemical Engineers' Handbook*, 9th Edition. New York: McGraw-Hill Education, 2019.

[24] R. G. M. van der Sman, I. A. F. van den Hoek, and Y. Zhao, "Interaction of milk fat solidification and cheese cooling," *J Food Eng*, vol. 395, p. 112531, Jul. 2025, doi: 10.1016/j.jfoodeng.2025.112531.